MNRAS 000, 1-6 (2017) Preprint 7 December 2021 Compiled using MNRAS LATEX style file v3.0

Evidence for photoionization-driven variability in narrow absorption lines

Wei-Jian Lu,[1⋆] Ying-Ru Lin,[1⋆] Yi-Ping Qin,[1,2]Wei-Rong Huang,[2]Cai-Juan Pan,[1] Hong-Yan Huang,[1]Min Yao,[1]Wei-Jing Nong,[1]Zhi-Kao Yao,[1]Mei-Mei Lu,[1] Da-Sheng Pan,[1]Hong-Qiang Huang,[1]and Qing-Lin Han[1]
[1]*Dapartment of Physics and Telecommunication Engineering, Baise University, Baise 533000, China*
[2]*Center for Astrophysics, Guangzhou University, Guangzhou 510006, China*

arXiv:1706.00602v1 [astro-ph.GA] 2 Jun 2017

Accepted XXX. Received YYY; in original form ZZZ

ABSTRACT
In this Letter, we report the discovery of a strong correlation between the variability of narrow absorption lines (NALs) and the ionizing continuum from a two-epoch spectra sample of 40 quasars containing 52 variable C IV $\lambda\lambda$1548, 1551 absorption doublets. According to the concordance index, this sample is classified into two subsamples. Subsample I shows an anti-correlation between the variations of absorption lines and the continuum, while Subsample II exhibits a positive correlation. These results imply that these variable C IV $\lambda\lambda$1548, 1551 absorption doublets are intrinsic to the corresponding quasars and that their variations are caused primarily by the fluctuations of the ionizing continuum. Based on our analysis, we propose that there might be two kinds of absorption gas: one that is very sensitive to the continuum variations, the another that is not. In addition, we suggest that in many cases the emergence or disappearance of NALs is caused by fluctuations of the ionizing continuum.

Key words: galaxies : active – quasars : absorption lines – quasars: general.

1 INTRODUCTION

The absorption lines in quasar spectra can place constraints on the basic properties of quasar environments and be used to probe the gaseous content of the Universe from early cosmic times to the present day. According to their origins, quasar absorption lines are divided into two classes. Intrinsic absorption lines are thought to be produced by the gas directly associated with the quasar central region or by that in the host galaxy, while intervening absorption lines are caused by foreground galaxies along the line of sight to the background quasar. Based on the absorption width of their profiles, intrinsic absorption lines can be further classified into broad absorption lines (BALs: absorption widths of at least 2000 km s^{-1}, e.g. Weymann et al. 1991), narrow absorption lines (NALs: absorption widths of a few hundred km s^{-1}) and mini-broad absorption lines (mini-BALs: absorption widths between BALs and NALs; e.g. Hamann & Sabra 2004).

Previous observations have found variations (both in strength and in shape) in quasar BALs/mini-BALs on timescales ranging from a few years to a few months in the quasar rest-frame (e.g. Filiz Ak et al. 2012, 2013; Welling et al. 2014; Misawa, Charlton & Eracleous 2014; Wang et al. 2015, and references therein), and similar variations in NALs (e.g. Hamann et al. 1995; Barlow, Hamann & Sargent 1997; Hamann, Barlow & Junkkarinen 1997; Ganguly, Charlton & Eracleous 2001b; Narayanan et al. 2004; Wise et al. 2004; Misawa et al. 2005; Hamann et al. 2011; Chen et al. 2013, 2015; Chen & Qin 2015). The time variability of absorption lines may be caused by the bulk motion of the absorbing gas across the line of sight (e.g., Hamann et al. 2008; Krongold, Binette & Hernndez-Ibarra 2010; Hall et al. 2011; Capellupo et al. 2013; Chen et al. 2013; Shi et al. 2016; Rogerson et al. 2016) or by changes in the ionization of the gas (e.g., Hamann et al. 2011; Filiz Ak et al. 2013; Arav et al. 2015; Chen & Qin 2015; Wang et al. 2015). Which mechanism is the main cause of the absorption-line variability is still under debate.

Research into the correlation between variations in absorption lines and the continuum is a method that has been proposed for determining the origin of the absorption-line variability. In fact, some researches into the correlations between variations of BALs and the continuum/emission has already been carried out. A few papers reported that no clear correlation between the variation of BALs and the continuum (Gibson et al. 2008; Wildy et al. 2014; Vivek et al. 2014) has ever been detected, while several recent studies

⋆ E-mail:william_lo@qq.com; yingru_lin@qq.com

© 2017 The Authors

have provided evidence of the coordinated variations between BALs and the continuum (Capellupo et al. 2012; Filiz Ak et al. 2012, 2013; Misawa et al. 2014; Wang et al. 2015). Although there are no reports on the correlation between the variability of NALs and the continuum, recent researches based on combining multi-epoch high-resolution UV and X-ray data for the Seyfert galaxy NGC 5548 showed a definitive case of NAL variation caused by photoionization changes (Kaastra et al. 2014, Arav et al. 2015), and well-coordinated variations of different absorption systems between different epochs have been detected in individual quasars (Hamann et al. 2011; Chen & Qin 2015).

In this paper, we study the correlation between the variations of C IV NALs and those of the continuum. We describe the sample of spectra in Section 2 and perform statistical analyses in Section 3. The discussion is presented in Section 4, and conclusions are provided in Section 5.

2 SPECTRAL SAMPLE

The Sloan Digital Sky Survey (SDSS; York et al. 2000) is a project that aims to obtain detailed three-dimensional maps of a large area of the Universe using a 2.5-m telescope (Gunn et al. 2006). The first three periods of the survey in the SDSS project have been completed. The Baryon Oscillation Spectroscopic Survey (BOSS; Eisenstein et al. 2011) is one of the programs in the third period of SDSS (SDSS-III, Eisenstein et al. 2011; Pâris et al. 2012). SDSS-I/II spectra have a spectral resolution of R≈1800-2200 (e.g. York et al. 2000), while BOSS spectra have a resolution of R≈ 1300-2500 (Pâris et al. 2012).

Using the sample of 7932 quasars observed by both SDSS-I/II (Data Release 7; Schneider et al. 2010) and BOSS (Data Release 9; Pâris et al. 2012), Chen et al. (2015) presented a catalogue of 52 pairs of obviously variable C IV $\lambda\lambda$1548, 1551 absorption doublets (with confident levels of >4σ for λ 1548 lines and >3σ for λ 1551 lines), identified from 40 quasar spectra. In the catalogue of variable C IV absorption doublets, there are 24 systems that have emerged in or disappeared from the latter spectra. The two SDSS observations span timescales ΔMJD = 304–1416 d in the quasar rest-frame. The range of the emission redshift of these quasars is $z_{\rm em}$ = 1.8–3.5, while that of the absorption redshift of the 52 C IV $\lambda\lambda$1548, 1551 absorption doublets is $z_{\rm abs}$ = 1.7–3.3. All of the 40 quasars have a signal-to-noise ratio (SNR) ≥8.0 for both SDSS-I/II and BOSS spectra (Chen et al. 2015).

In the following, we will study the correlation between the variations of NALs and those of the continuum using the above sample consisting of the two-epoch spectra of the 40 quasars.

3 CORRELATION ANALYSIS AND RESULTS

3.1 Distribution of the concordance index for C IV NALs against the continuum

Adopting the method used by Wang et al. (2015), we consider that the continuum varies significantly when the fluctuation of the continuum flux at ∼1450 Å (in the quasar rest-frame) is more than 5 per cent between the two observations. In this section, the variations of the equivalent widths (EWs) of C IV absorption lines are taken directly from Chen et al. (2015). According to Wang et al. (2015), we define a concordance index of +1 for the cases in which both the absorption line and the continuum become stronger or both of them become weaker, of −1 when they vary in the opposite way, and of 0 when the continuum has no significant variation. The distribution of the concordance index is shown in Fig. 1.

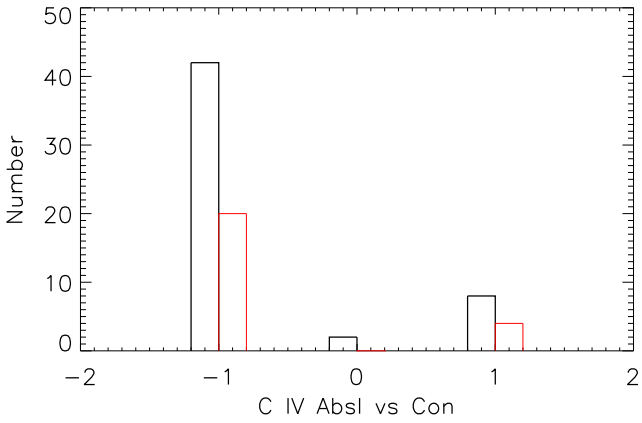


Figure 1. Count distribution of the concordance index for C IV NALs against the continuum. A concordance index of +1 represents the cases where both the absorption line and the continuum become stronger or both of them become weaker, one of −1 represents the opposite cases, and one of 0 represents the case in which the continuum does not change significantly between the two SDSS observations. The black boxes show the distribution of all spectrum pairs in our sample, while the red boxes show the distribution of the spectrum pairs of the emergence or disappearance of C IV NALs.

As depicted in Fig. 1, the variations of absorption-line EWs are highly statistically coordinated with the variations of the continuum flux. More specifically, about 81 per cent of the C IV absorption lines weaken when the continuum brightens, or the absorption lines strengthen while the continuum dims (the case when the concordance index is −1); about 15 per cent of the C IV absorption lines strengthen when the continuum brightens, or the absorption lines weaken while the continuum dims (the case when the concordance index is +1); the remaining two quasars have no significant continuum variations between the two epochs of observations. Note that a highly level of coordination is also detected from the spectrum pairs of the emerged or disappeared events of C IV NALs.

3.2 Correlation analysis between C IV NALs and the continuum

Based on the concordance index, we extracted three subsamples from the whole sample. Subsample I includes the spectrum pairs with a concordance index of −1. Subsample II includes those with a concordance index of +1. Subsample III contains the spectrum pairs of the emergence or disappearance of C IV NALs included in Subsample I. In the following, we analyse the correlation between the variations of C IV absorption-line EWs and those of the continuum flux

Table 1. C IV absorption systems and the continuum data.

SDSS NAME	z_{em}[a]	z_{abs}[b]	F_{cont1}[c]	F_{cont2}[c]	ΔF_{cont}	ΔEW_r48	ΔEW_r51	Index[d]	Note[b]
005157.24+000354.7	1.9609	1.8681	31.14 ± 1.51	19.60 ± 0.78	−0.23 ± 0.03	0.79 ± 0.25	0.64 ± 0.50	−1	Emerged
015017.70+002902.4	3.0013	2.8344	6.86 ± 0.83	5.27 ± 0.38	−0.13 ± 0.07	0.74 ± 0.35	0.72 ± 0.31	−1	Emerged
020629.33+004843.1	2.4988	2.3624	12.26 ± 1.05	5.88 ± 0.32	−0.35 ± 0.05	0.78 ± 0.39	0.76 ± 0.23	−1	Emerged
024304.68+000005.4	2.0069	1.9426	12.71 ± 1.65	19.80 ± 1.06	0.22 ± 0.07	−0.29 ± 0.05	−0.23 ± 0.07	−1	Weakened
073232.79+435500.4	3.4618	3.2569	7.48 ± 0.57	5.83 ± 0.33	−0.12 ± 0.05	0.80 ± 0.28	0.55 ± 0.20	−1	Strengthened
073406.75+273355.6	1.9239	1.8609	93.78 ± 2.68	83.53 ± 2.13	−0.06 ± 0.02	0.21 ± 0.05	0.34 ± 0.05	−1	Strengthened
080006.59+265054.7	2.3438	2.3033	10.23 ± 0.92	5.11 ± 0.48	−0.33 ± 0.06	0.67 ± 0.24	0.71 ± 0.38	−1	Emerged
080609.24+141146.4	2.2877	2.0062	19.14 ± 0.98	16.97 ± 0.55	−0.06 ± 0.03	−0.93 ± 0.19	−0.81 ± 0.18	1	Disappeared
080906.88+172955.1	2.9770	2.8828	14.23 ± 1.05	11.41 ± 0.43	−0.11 ± 0.04	0.71 ± 0.19	0.85 ± 0.88	−1	Emerged
080906.88+172955.1	2.9770	2.9384	14.23 ± 1.05	11.41 ± 0.43	−0.11 ± 0.04	0.63 ± 0.13	0.59 ± 0.11	−1	Strengthened
081655.49+455633.7	2.7168	2.5745	7.01 ± 0.78	7.99 ± 0.24	0.07 ± 0.06	0.68 ± 0.32	0.66 ± 0.25	1	Emerged
081929.59+232237.4	1.8467	1.7258	34.28 ± 1.39	22.85 ± 1.01	−0.20 ± 0.03	−0.49 ± 0.14	−0.52 ± 0.15	1	Weakened
082751.78+132107.2	1.8289	1.8019	42.91 ± 1.91	35.98 ± 1.18	−0.09 ± 0.03	0.17 ± 0.04	0.18 ± 0.05	−1	Strengthened
091621.46+010015.4	2.2255	2.1264	12.72 ± 0.84	9.15 ± 0.49	−0.16 ± 0.04	0.78 ± 0.30	0.70 ± 0.20	−1	Emerged
091621.46+010015.4	2.2255	2.1629	12.72 ± 0.84	9.15 ± 0.49	−0.16 ± 0.04	0.36 ± 0.05	0.26 ± 0.04	−1	Strengthened
091621.46+010015.4	2.2255	2.1741	12.72 ± 0.84	9.15 ± 0.49	−0.16 ± 0.04	0.40 ± 0.07	0.46 ± 0.11	−1	Strengthened
095254.10+021932.8	2.1526	2.0056	19.11 ± 1.15	21.37 ± 0.71	0.06 ± 0.03	0.67 ± 0.32	0.81 ± 0.50	1	Emerged
100716.69+030438.7	2.1241	1.9129	25.40 ± 1.20	16.00 ± 0.73	−0.23 ± 0.03	0.23 ± 0.05	0.35 ± 0.05	−1	Strengthened
100716.69+030438.7	2.1241	1.9426	25.40 ± 1.20	16.00 ± 0.73	−0.23 ± 0.03	0.86 ± 0.15	0.83 ± 0.27	−1	Emerged
103115.69+374849.5	2.2590	2.2100	8.24 ± 0.94	9.98 ± 0.51	0.10 ± 0.06	−0.78 ± 0.16	−0.75 ± 0.29	−1	Disappeared
103115.69+374849.5	2.2590	2.2253	8.24 ± 0.94	9.98 ± 0.51	0.10 ± 0.06	−0.77 ± 0.25	−0.85 ± 0.17	−1	Disappeared
103842.14+350906.9	2.2049	2.1563	13.52 ± 1.25	7.97 ± 0.48	−0.26 ± 0.05	0.35 ± 0.08	0.34 ± 0.08	−1	Strengthened
104841.02+000042.8	2.0246	1.9468	12.62 ± 1.02	13.87 ± 0.63	0.05 ± 0.05	−0.54 ± 0.08	−0.52 ± 0.11	−1	Weakened
104923.94+012224.6	1.9454	1.9087	37.98 ± 2.16	17.72 ± 0.79	−0.36 ± 0.03	0.74 ± 0.10	0.67 ± 0.13	−1	Strengthened
105207.90+362219.4	2.3157	2.2666	10.94 ± 1.13	14.78 ± 0.66	0.15 ± 0.06	0.32 ± 0.08	0.65 ± 0.15	1	Strengthened
110726.04+385158.2	2.6603	2.6134	13.70 ± 0.43	11.57 ± 0.55	−0.08 ± 0.03	−0.23 ± 0.05	−0.20 ± 0.07	1	Weakened
115122.14+020426.3	2.4085	2.3269	14.06 ± 1.02	7.88 ± 0.60	−0.28 ± 0.05	0.58 ± 0.10	0.52 ± 0.11	−1	Strengthened
115122.14+020426.3	2.4085	2.3742	14.06 ± 1.02	7.88 ± 0.60	−0.28 ± 0.05	0.18 ± 0.04	0.14 ± 0.04	−1	Strengthened
120819.29+035559.4	2.0213	1.9500	22.48 ± 1.88	12.93 ± 0.59	−0.27 ± 0.05	0.17 ± 0.04	0.26 ± 0.05	−1	Strengthened
123720.85-011314.9	2.1620	2.1283	10.22 ± 1.24	7.52 ± 0.46	−0.15 ± 0.07	0.78 ± 0.13	0.66 ± 0.17	−1	Strengthened
124829.46+341231.3	2.2285	2.0621	18.65 ± 1.24	8.88 ± 0.54	−0.35 ± 0.04	0.84 ± 0.20	0.87 ± 0.50	−1	Emerged
124829.46+341231.3	2.2285	2.0769	18.65 ± 1.24	8.88 ± 0.54	−0.35 ± 0.04	0.86 ± 0.30	0.83 ± 0.55	−1	Emerged
125216.58+052737.7	1.9034	1.8155	52.57 ± 2.29	88.82 ± 2.30	0.26 ± 0.02	−0.80 ± 0.22	−0.81 ± 0.12	−1	Disappeared
125216.58+052737.7	1.9034	1.8638	52.57 ± 2.29	88.82 ± 2.30	0.26 ± 0.02	−0.90 ± 0.06	−0.87 ± 0.18	−1	Disappeared
125216.58+052737.7	1.9034	1.8831	52.57 ± 2.29	88.82 ± 2.30	0.26 ± 0.02	−0.57 ± 0.03	−0.53 ± 0.05	−1	Weakened
125216.58+052737.7	1.9034	1.8946	52.57 ± 2.29	88.82 ± 2.30	0.26 ± 0.02	−0.75 ± 0.05	−0.76 ± 0.10	−1	Weakened
132333.03+004750.2	1.7785	1.7701	29.60 ± 2.69	34.12 ± 1.48	0.07 ± 0.05	−0.02 ± 0.04	−0.01 ± 0.04	−1	Weakened
134544.55+002810.7	2.4641	2.3514	11.21 ± 1.10	14.86 ± 0.54	0.14 ± 0.05	−0.87 ± 0.11	−0.89 ± 0.11	−1	Disappeared
134544.55+002810.7	2.4641	2.3686	11.21 ± 1.10	14.86 ± 0.54	0.14 ± 0.05	−0.93 ± 0.08	−0.90 ± 0.11	−1	Disappeared
134544.55+002810.7	2.4641	2.3964	11.21 ± 1.10	14.86 ± 0.54	0.14 ± 0.05	−0.40 ± 0.05	−0.54 ± 0.06	−1	Weakened
140815.58+060023.3	2.5830	2.5519	7.28 ± 0.80	4.80 ± 0.38	−0.20 ± 0.07	0.86 ± 0.75	0.85 ± 0.31	−1	Emerged
150033.53+003353.6	2.4360	2.1849	13.23 ± 1.04	18.97 ± 0.63	0.18 ± 0.04	0.62 ± 0.41	0.68 ± 0.25	1	Emerged
160445.92+335759.0	1.8776	1.7709	11.05 ± 1.41	9.34 ± 0.62	−0.08 ± 0.07	0.69 ± 0.39	0.75 ± 0.25	−1	Emerged
160613.99+314143.4	2.0569	2.0240	11.22 ± 1.21	10.72 ± 0.64	−0.02 ± 0.06	−0.35 ± 0.07	−0.41 ± 0.08	0	Weakened
161336.81+054701.7	2.4855	2.4152	9.03 ± 0.83	8.55 ± 0.46	−0.03 ± 0.05	0.66 ± 0.28	0.68 ± 0.27	−1	Emerged
161511.35+314728.3	2.0981	1.9157	41.00 ± 1.80	34.78 ± 1.11	−0.08 ± 0.03	−0.16 ± 0.04	−0.25 ± 0.05	1	Weakened
162701.94+313549.2	2.3263	2.2785	65.53 ± 2.40	62.42 ± 1.46	−0.02 ± 0.02	0.13 ± 0.03	0.25 ± 0.03	0	Strengthened
162935.68+321009.5	2.0364	1.9345	12.72 ± 1.44	9.55 ± 0.65	−0.14 ± 0.07	0.43 ± 0.13	0.35 ± 0.11	−1	Strengthened
212943.25+003005.6	2.6802	2.5726	8.11 ± 0.91	6.52 ± 0.36	−0.11 ± 0.06	0.77 ± 0.39	0.72 ± 0.18	−1	Emerged
213648.17-001546.6	2.1736	1.8372	8.35 ± 1.03	14.62 ± 0.57	0.27 ± 0.06	−0.89 ± 0.12	−0.86 ± 0.26	−1	Disappeared
222157.97-010331.0	2.6744	2.5459	15.66 ± 0.74	16.86 ± 0.51	0.04 ± 0.03	−0.31 ± 0.04	−0.34 ± 0.05	−1	Weakened
230034.04-004901.5	2.2125	2.1422	8.07 ± 0.95	13.67 ± 0.60	0.26 ± 0.06	−0.62 ± 0.07	−0.28 ± 0.07	−1	Weakened

Notes.[a]Following Chen et al. (2015), the value of z_{em} is taken from Hewett & Wild (2010).
[b]The value of z_{abs} and the contents of "Note" are directly taken from Chen et al. (2015).
[c]The values of F_{noise1} and F_{noise2} are measured in units of 10^{-17} erg cm^{-2} s^{-1} $^{-1}$.
[d]The concordance index.

for the whole sample and the above three subsamples, respectively.

Following Chen et al. (2015), we fitted a pseudo-continuum for each spectrum using a combination of cubic spline functions and Gaussian functions. Then we evaluated the pseudo-continuum fitting flux variability amplitude between two observations for each quasar using

$$\Delta F_{cont} = \frac{F_{cont2} - F_{cont1}}{|F_{cont2}| + |F_{cont1}|}, \quad (1)$$

where F_{cont1} and F_{cont2} denote the flux of the pseudo-continuum at ∼ 1450 Å in the quasar rest-frame for the earlier and later epochs, respectively. The propagation of

the error for $\Delta F_{\rm cont}$ can be evaluated using

$$\sigma_{\Delta F_{\rm cont}} = \sqrt{(\frac{\partial \Delta F_{\rm cont}}{\partial F_{\rm cont1}})^2 {F_{\rm noise1}}^2 + (\frac{\partial \Delta F_{\rm cont}}{\partial F_{\rm cont2}})^2 {F_{\rm noise2}}^2}, \quad (2)$$

where $F_{\rm noise1}$ and $F_{\rm noise2}$ are the flux uncertainties for the earlier and later SDSS epochs.

Then we calculated the variability amplitude of EWs between the two SDSS observations for the bluer and redder members ($\Delta EW_{\rm r}48$ and $\Delta EW_{\rm r}51$) for each C IV $\lambda\lambda$1548, 1551 doublet using

$$\Delta EW_{\rm r}48(51) = \frac{EW_{\rm r}48(51)_2 - EW_{\rm r}48(51)_1}{|EW_{\rm r}48(51)_2| + |EW_{\rm r}48(51)_1|}, \quad (3)$$

where the EWs for C IV λ1548 and C IV λ1551 were taken directly from Chen et al. (2015). We also calculated their corresponding errors ($\sigma_{\Delta EW_{\rm r}48}$ and $\sigma_{\Delta EW_{\rm r}51}$) with the same method as used in calculating $\sigma_{\Delta F_{\rm cont}}$, respectively. The parameters and estimated values are listed in Table 1.

Here, we present plots of $\Delta EW_{\rm r}48$ and $\Delta EW_{\rm r}51$ versus $\Delta F_{\rm cont}$ for all objects (Fig. 2). Linear functions are adopted to fit the data for the whole sample and the three subsamples, respectively. The statistical parameters are listed in Table 2.

4 DISCUSSION

4.1 Properties of the variable C IV $\lambda\lambda$1548, 1551 absorption doublets

We believe that the variable absorption systems in our sample are intrinsic to the corresponding quasars. On the one hand, the result of the time variability analysis in this paper, namely the fact the variations of narrow C IV absorption lines show a significantly correlative with the continuum variations, strongly supports the above suggestion. On the other hand, the time variability of intervening cloud structures would not be expected on such short time-scales because of their large sizes and low densities (e.g., Hamann et al. 1995).

Based on the time variability analysis of 12 intrinsic NALs and seven mini-BALs within the timescale of 1–3.5 yr in the quasar rest-frame, Misawa et al. (2014) found that only the latter show significant variability. These authors suggested that changes in both the ionizing continuum and the partial coverage can lead to the variability of mini-BALs, and that the latter mechanism is the main driver of NAL variability. However, our statistical analysis shows a significant anti-correlation between the variation of narrow C IV absorption lines and that of the pseudo-continuum flux (see Fig. 2), implying that the NAL variability is caused primarily by fluctuations in the ionizing continuum.

More specifically, we find that our sample of variable absorption lines can be divided mainly into two subsamples according to the concordance index. Subsample I (∼81 per cent) shows an anti-correlation between the variability of NALs and the continuum while Subsample II (∼15 per cent) shows a positive correlation. This phenomenon could be explained by the different ionization states of the absorbers (Wang et al. 2015; Lu et al. in preparation).

4.2 On the emergence or disappearance of C IV $\lambda\lambda$1548, 1551 absorption doublets

In our sample, there are 24 C IV $\lambda\lambda$1548, 1551 absorption doublets that emerged in or disappeared from the BOSS spectra (Chen et al. 2015), of which 20 absorption systems have a concordance index of −1 (which are classified as Subsample III).

It is evident from Fig. 2 that this population is bimodal. The points with positive values of $\Delta EW_{\rm r}48(51)$ have values between 0.62 and 0.87, while the points with negative values of $\Delta EW_{\rm r}48(51)$ have values between –0.75 to –0.93. We find that the population distributes a narrow-value range of $\Delta EW_{\rm r}48(51)$ near –0.7 to –0.9 or 0.7 to 0.9. According to equation (3), $\Delta EW_{\rm r}48(51)$ in Subsample III should be +1 or −1. The deviations arise because, even in these extreme cases where no absorption lines are observed, considering the error of EWs between SDSS I/II and BOSS spectra, Chen et al. (2015) still allow a try of fit to the 'imagined' absorption troughs. As a result, a value of EWs is obtained that is slightly greater than zero instead of being zero. Therefore, we find that the values of $\Delta EW_{\rm r}48(51)$ in Subsample III are slightly lower than +1 or slightly greater than −1. The observed bimodal population is expected, because while one group is associated with the case of emergence, the other group corresponds to the case of disappearance (note that the two groups represent extreme cases of the corresponding variations).

In addition, it can be seen that the data points for Subsample III span all values of $\Delta F_{\rm cont}$. This suggests that the emergence as well as the disappearance of NALs do not always require that the continuum varies considerably, but, instead, emergence or disappearance could occur for even small variations. This implies that some absorption gas is very sensitive to continuum variations, which was also suggested for the case of BALs (Filiz Ak et al. 2013; Wang et al. 2015). We therefore suggest that there might be two kinds of absorption gas: one that is very sensitive to the continuum variations (which is expected to yield data such as that in Subsample III), and aonther that is not so sensitive (which is expected to produce the type of data other than that in Subsample III). In Fig. 2, it is obvious that the best linear fitting for Subsample III provides the steepest slope for all points in the whole sample (this is to be expected, because data in Subsample III reflect extreme cases of variation). Although some cases of the emergence or disappearance of NALs might be caused by the bulk motion of the absorption gas (Chen et al. 2013), the significant anti-correlation between $\Delta EW_{\rm r}48(51)$ and $\Delta F_{\rm cont}$ for Subsample III (see Fig. 2) strongly implies that many extreme variations of NALs must also be due to the fluctuations of the ionizing continuum.

It is clear that separate linear fits for the two extreme groups (corresponding to the emergence or disappearance cases) in Subsample III will produce very weak correlation between $\Delta EW_{\rm r}48(51)$ and $\Delta F_{\rm cont}$. This is to be expected, because for one group the value of $\Delta EW_{\rm r}48(51)$ is expected to be +1, while it is expected to be −1 for the other group. When ignoring the data of both of groups, there is still a significant anti-correlation between the two quantities ($r = -0.837$, $P < 0.001$), suggesting that the existence of this bimodal data of Subsample III strengthens the relationship of the anti-correlation but the relationship itself is quite robust.

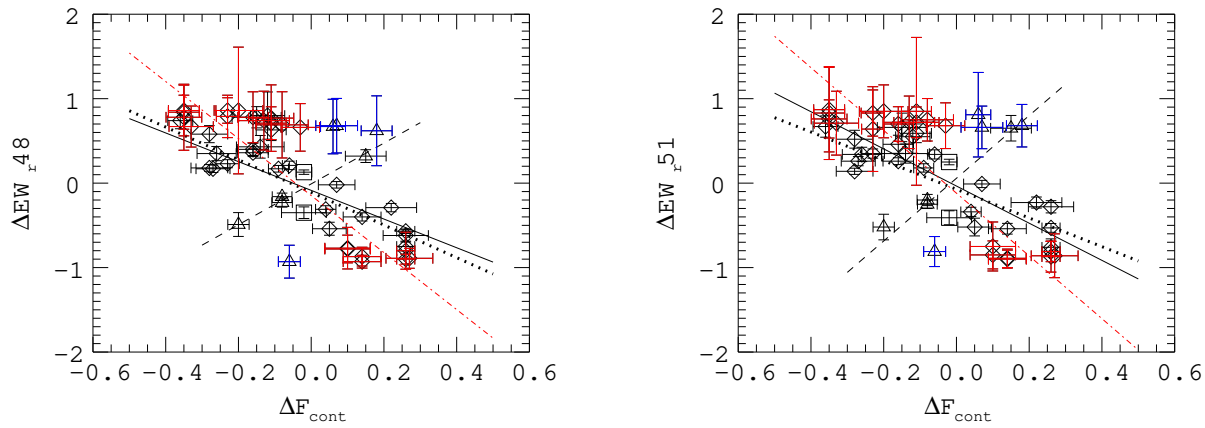


Figure 2. Plots of the variability amplitudes of narrow C IV absorption lines and the pseudo-continuum (left panel: C IV λ1548 versus the pseudo-continuum; right panel: C IV λ1551 versus the pseudo-continuum). The black rhombuses, black triangles and black squares represent the data with concordance indexes of −1, +1 and 0, respectively. The black solid line, black dotted line, black dashed line and red dot-dashed line are the best linear fits for the whole sample, Subsample I, Subsample II and Subsample III, respectively. The errors are shown by the error bars. The data with red error bars are Subsample III. The data with blue error bars are the spectrum pairs of emerging or disappearing absorption lines in Subsample II.

Table 2. Correlated parameters of $\Delta EW_{\rm r}48$ ($\Delta EW_{\rm r}51$) vs. $\Delta F_{\rm cont}$ for the whole sample and each subsample. The data in brackets denote the results of $\Delta EW_{\rm r}51$ vs. $\Delta F_{\rm cont}$.

	The whole sample	Subsample I	Subsample II	Subsample III
N[a]	52	42	8	20
r[b]	–0.699(–0.661)	–0.859(–0.848)	0.778(0.850)	–0.901(–0.893)
P[c]	<0.001(<0.001)	<0.001(<0.001)	<0.05(<0.01)	<0.001(<0.001)
k[d]	−1.699 ± 0.067(−2.200 ± 0.028)	−1.933 ± 0.067(−1.697 ± 0.068)	2.417 ± 0.325(3.714 ± 0.485)	−3.376 ± 0.177(−3.715 ± 0.247)
b[e]	−0.086 ± 0.012(−0.034 ± 0.005)	−0.109 ± 0.011(−0.073 ± 0.013)	−0.009 ± 0.033(0.058 ± 0.047)	−0.147 ± 0.039(−0.119 ± 0.048)

Notes.[a] The number of absorption systems in the samples.
[b] The linear Pearson correlation coefficient.
[c] The significance level of the Pearson correlation coefficient.
[d] The slope of the best linear fit.
[e] The intercept of the best linear fit.

4.3 Comparison of NAL and BAL/mini-BAL variability

We found that the variability of NALs is significantly correlated with the continuum variability. However, as noted in the Introduction, such a strong correlation between the variability of BALs/mini-BALs and the continuum has not yet been found (although coordinated variations between them have been detected; see Wang et al. 2015). A plausible explanation for the different reactions between BALs/mini-BALs and NALs is that BAL/mini-BAL outflows may correspond to relatively larger clumpy/filament structures, whose UV resonance doublets are usually blended and saturated, while the NALs are caused by the smaller and lower-density portion of the outflow wind (Murray et al. 1995; Proga, Stone & Kallman 2000; Elvis 2000; Ganguly et al. 2001a; Hall et al. 2007; Misawa et al. 2014), so that NALs may be more sensitive than BALs regarding responses to the continuum variability.

5 CONCLUSION

We have studied the correlation between the NAL variability and the continuum variability using a sample of two-epoch SDSS spectra of 40 quasars with 52 variable narrow-absorption systems. We analysed quantitatively the variability amplitude of EWs of C IV absorption lines and that of the continuum flux and found a significant correlation between them. As hinted at by the statistical results, we propose that the changes of the C IV $\lambda\lambda$1548, 1551 absorption doublets in our sample are driven mainly by the fluctuations of the ionizing continuum.

Our analysis suggests that the emergence and disappearance of NALs does not require that the continuum must vary considerably. Instead, these phenomena could occur for any level of variation of the continuum. We suggest that there might be two kinds of absorption gas: one that is very sensitive to the continuum variations, and another that is not. Based on Fig. 2, we believe that many cases of the emergence or disappearance of NALs are caused by fluctuations of the ionizing continuum as well.

ACKNOWLEDGEMENTS

We thank the anonymous referee for helpful comments. This work was supported by the Science Research Projects of Guangxi Colleges and Universities (No. KY2015YB289), and the Key Projects of Baise University (No. 2015KAN04).

Funding for SDSS-III was provided by the Alfred P. Sloan Foundation, the Participating Institutions, the National Science Foundation, and the US Department of Energy Office of Science. The SDSS-III web site is http://www.sdss 3.org/.

SDSS-III is managed by the Astrophysical Research Consortium for the Participating Institutions of the SDSS-III Collaboration, including the University of Arizona, the Brazilian Participation Group, Brookhaven National Laboratory, Carnegie Mellon University, University of Florida, the French Participation Group, the German Participation Group, Harvard University, the Instituto de Astrofisica de Canarias, the Michigan State/Notre Dame/JINA Participation Group, Johns Hopkins University, Lawrence Berkeley National Laboratory, Max Planck Institute for Astrophysics, Max Planck Institute for Extraterrestrial Physics, New Mexico State University, New York University, Ohio State University, Pennsylvania State University, University of Portsmouth, Princeton University, the Spanish Participation Group, University of Tokyo, University of Utah, Vanderbilt University, University of Virginia, University of Washington, and Yale University.

REFERENCES

Arav, N., et al., 2015, A&A, 577, 37
Barlow T. A., Hamann F., Sargent W. L. W., 1997, in Arav N., Shlosman I., Weymann R. J., eds, Astronomy Society of the Pacific Conference Series Vol. 128, Mass Ejection from Active Galactic Nuclei. Astron. Soc. Pac., San Francisco, p. 13
Capellupo D. M., Hamann F., Shields J. C., Rodrguez Hidalgo P., Barlow T. A., 2012, MNRAS, 422, 3249
Capellupo D. M., Hamann F., Shields J. C., Halpern J. P., Barlow T. A., 2013, MNRAS, 429, 1872
Chen Z.-F., Qin Y.-P., 2015, ApJ, 799, 63
Chen Z.-F., Li M.-S., Huang W.-R., Pan C.-J., Li Y.-B., 2013, MNRAS, 434, 3275
Chen Z.-F., Gu Q.-S., Chen Y.-M., Cao Y., 2015, MNRAS, 450, 3904
Eisenstein D. J. et al., 2011, AJ, 142, 72
Elvis M., 2000, ApJ, 545, 63
Filiz Ak N. et al., 2012, ApJ, 757, 114
Filiz Ak N. et al., 2013, ApJ, 777, 168
Ganguly R., Charlton J. C., Eracleous M., 2001a, ApJ, 556, L7
Ganguly R., Bond N. A., Charlton J. C., Eracleous M., Brandt W. N., Churchill C. W., 2001b, ApJ, 549, 133
Gibson R. R., Brandt W. N., Schneider D. P., Gallagher S. C., 2008, ApJ, 675, 985
Gunn J. E. et al., 2006, AJ, 131, 2332
Hall P. B., Sadavoy S. I., Hutsemekers D., Everett J. E., Rafiee A., 2007, ApJ, 665, 174
Hall P. B., Anosov K., White R. L., Brandt W. N., Gregg M. D., Gibson R. R., Becker R. H., Schneider D. P., 2011, MNRAS, 411, 2653
Hamann F., Sabra B., 2004, in Richards G. T., Hall P. B., eds, Astronomy Society of the Pacific Conference Series Vol. 311. AGN Physics with the Sloan Digital Sky Survey. Astron. Soc. Pac., San Francisco, p. 203
Hamann F., Barlow T. A., Beaver E. A., Burbidge E. M., Cohen R. D., Junkkarinen V., Lyons R., 1995, ApJ, 443, 606
Hamann F., Barlow T. A., Junkkarinen V., 1997, ApJ, 478, 87
Hamann F., Kaplan K. F., Rodrguez Hidalgo P., Prochaska J. X., Herbert-Fort S., 2008, MNRAS, 391, L39
Hamann F., Kanekar N., Prochaska J. X., Murphy M.T., Ellison S., Malec A.L., Milutinovic N., Ubachs W., 2011, MNRAS, 410, 1957
Hewett P. C., Wild V., 2010, MNRAS, 405, 2302
Kaastra J. S. et al., 2014, Science, 345, 64
Krongold Y., Binette L., Hernndez-Ibarra F., 2010, ApJ, 724, L203
Misawa T., Eracleous M., Charlton J. C., Tajitsu A., 2005, ApJ, 629, 115
Misawa T., Charlton J. C., Eracleous M., 2014, ApJ, 792, 77
Murray N., Chiang J., Grossman S. A., Voit G. M., 1995, ApJ, 451, 498
Narayanan D., Hamann F., Barlow T., Burbidge E. M., Cohen R. D., Junkkarinen V., Lyons R., 2004, ApJ, 601, 715
Pâris I. et al., 2012, A&A, 548, 66
Proga D., Stone J. M., Kallman T. R., 2000, ApJ, 543, 686
Rogerson J. A., Hall P. B., Hidalgo P.R., Pirkola P., William N.B., Filiz Ak N., 2016, MNRAS, 457, 405
Schneider D. P. et al., 2010, AJ, 139, 2360
Shi X.-H., et al., 2016, ApJ, 819, 99
Vivek M., Srianand R., Petitjean P., Mohan V., Mahabal A., Samui S., 2014, MNRAS, 440, 799
Wang T.-G., Yang C.-W., Wang H.-Y., Ferland G., 2015, ApJ, 814, 150
Welling C. A., Miller B. P., Brandt W. N., Capellupo D. M., Gibson R. R., 2014, MNRAS, 440, 2474
Weymann R. J., Morris S. L., Foltz C. B., Hewett P. C. 1991, ApJ, 373, 23
Wildy C., Goad M. R., Allen J. T., 2014, MNRAS, 437, 1976
Wise J. H., Eracleous M., Charlton J. C., Ganguly R., 2004, ApJ, 613, 129
York D. G. et al, 2000, AJ, 120, 1579

This paper has been typeset from a TEX/LATEX file prepared by the author.